Stability of Nematic and Smectic Phases in Rod-Like Mesogens with Orientation−Dependent Attractive Interactions

B. Martínez-Haya*

Departamento de Sistemas Físicos, Químicos y Naturales, Universidad Pablo de Olavide, 41013 Seville, Spain

A. Cuetos

Soft Condensed Matter Group, Utrecht University, 3584 CC Utrecht, The Netherlands

Received: February 23, 2007; In Final Form: May 17, 2007

The stability of isotropic (I), nematic (N), smectic A (Sm A), and hexatic (Hex) liquid crystalline phases is studied for a fluid of molecules with a rod-like shape and dispersive interactions dependent on orientation. The fluid is modeled with the spherocylindrical Gay−Berne−Kihara interaction potential proposed in a recent work, with parameters favoring parallel pair orientations. The liquid crystal phase diagram is characterized for different molecular aspect ratios by means of Monte Carlo simulations in the isobaric−isothermal ensemble. Three types of triple points are observed, namely, I−Sm A−Hex, I−N−Sm A, and N−Sm A−Hex, leading to island-shape domains for the smectic A phase. The resulting phase diagrams are compared with those derived previously for prolate fluids of ellipsoidal and spherocylindrical symmetry. It is concluded that the stability of the layered phases with respect to the nematic phase is enhanced in the spherocylindrical fluids due to geometrical constraints. Furthermore, the anisotropy of the dispersive interactions induces a stronger dependence of the overall phase diagram on temperature and aids in the energetic stabilization of the hexatic crystalline phase with respect to the fluid smectic A phase.

I. Introduction

Computer simulation constitutes nowadays one of the most productive disciplines of material science. The comprehension of mesophasic behavior has to a great extent relied on the information provided by the different computational approaches of statistical mechanics.[1,2] Two recent reviews from Wilson[3] and Care and Cleaver,[4] devoted to the computer simulation of liquid crystals (LC), serve to illustrate the recent advances and the broad range of applications emerging from this field.

Since the first works on computer simulation of liquid crystals in the 1970s,[5] increasing efforts have been directed toward the extension of the accessible physical time and length scales. Of particular importance within this context has been the quest toward establishing realistic and yet simple molecular models that would guide in the rationalization and prediction of the physicochemical properties of specific mesogens.[1−3,6] Coarse-grain models have played a fundamental role in the field of liquid crystals. In their more accurate form, such models treat molecules with appropriate interaction centers at atomic resolution with a detailed treatment of the internal degrees of freedom. However, atomistic models have the disadvantage of becoming computationally expensive and, therefore, of imposing limitations to the size and time scale of the simulation system.[3,4] The alternative use of rigid molecular models has been successfully explored for the study of mesophases. Optimum rigid models should incorporate the relevant features of the excluded volume effects and molecular interactions, while keeping a reasonable analytical and computational efficiency for theoretical and simulation studies.

An important class of liquid crystalline systems is associated to molecules of roughly prolate axial symmetry. Different rigid models have been proposed in the past decades to describe these molecular fluids. Two types of molecular geometries have concentrated most of the efforts, namely ellipsoidal models and rod-like spherocylindrical or Kihara models. The simplest ellipsoidal models are the hard ellipsoid model[7] and the Gaussian-overlap model,[8] which have attracted renewed interest in past years.[9,10] The Gay−Berne potential (GB)[11] is the ellipsoidal model most extensively employed to study mesogenic behavior.[12−15] Remarkably, layered smectic phases are not stable in the purely repulsive ellipsoidal models, such as the hard ellipsoid fluid.[7,9,12,16,17] Smectic phases can be incorporated to the LC phase diagram with the introduction of specific attractive interactions to the ellipsoidal core.[15,18] On the other hand, Kihara models[19] constitute the most popular spherocylindrical fluids. The simplest Kihara potential, the hard spherocylinder model (HSC), already displays a rich LC behavior including nematic, smectic A, and solid phases, depending on molecular aspect ratio and thermodynamic conditions.[20,21] The analogous phase diagram for soft Kihara potentials has been investigated more recently.[22−25] Whereas the Kihara interaction model provides a closer description of the overall shape of rod-like molecules in comparison to their ellipsoidal counterparts, they present the intrinsic limitation of assigning the same interaction energies to a given molecular core distance, irrespectively of the relative orientations of the particles. This is in contrast with the interactions in real mesogens, where the dispersive forces tend to be greater for side-to-side pair configurations or, possibly, other arrangements if specific functional groups dominate the energetics.

In a previous work,[26] our group introduced a mesogenic pair potential which combines the more realistic features of the Kihara models (the spherocylindrical shape) and of the GB potential (the anisotropy in the strength of the interaction). The

10.1021/jp0715171 CCC: $37.00
Published on Web 06/26/2007

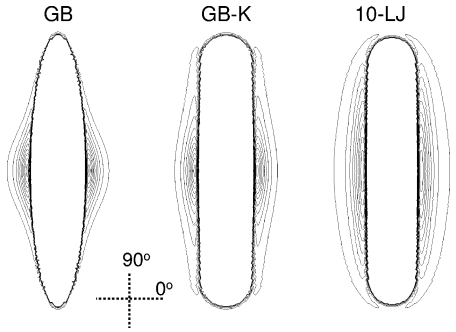

Figure 1. Equipotential energy surfaces for two parallel particles interacting through the spherocylindrical GB−K(5, 20, 1, 1) (i.e., with parameters $L^* = 4$, $\kappa = 5$, $\kappa' = 20$, $\mu = 1$, $\nu = 1$) potential (center), the ellipsoidal Gay−Berne GB(5, 20, 1, 1) potential (left) and a 10-site Lennard-Jones chain with the same aspect ratio (right). The position of the pair of particles is described by the polar coordinates (r_{ij}, θ), with $\theta = 0°$ for the side-to-side configuration and $\theta = 90°$ for the head-to-tail one. Note the qualitative resemblance of the multiple-site Lennard-Jones chain potential achieved with the GB−K model.

TABLE 1: Glossary of the Main Parameters Employed to Define the GB−K Fluid Model in Section II.A

parameters	definition
r_{ij}	vector joining the center-of-mass of particles i, j
u_k	director vector of particle k
d_m	minimum distance between the cores of particles i, j
ϵ_{GB} (r_{ij},u_i,u_j)	Gay−Berne term of the interaction potential
$U_K(d_m)$	Kihara term of the interaction potential
ϵ, k_B	energy scaling parameter and Boltzmann constant
L, σ	length and diameter of the cylindrical core
κ	molecular aspect ratio $\kappa = L/\sigma + 1$
κ', ν, μ	Gay−Berne parameters defining the interaction anisotropy
χ, χ'	$\chi = (\kappa^2 - 1)(\kappa^2 + 1)^{-1}$, $\chi' = (\kappa'^{1/\mu} - 1)(\kappa'^{1/\mu} + 1)^{-1}$

so-called Gay−Berne−Kihara potential (GB−K) provides a pair interaction qualitatively resembling that of a linear chain of Lennard-Jones centers (see Figure 1). Interestingly, a novel way to mimic elongated molecules with Lennard-Jones centers has been recently reported.[27] The Monte Carlo simulation study of ref 26 for the GB−K fluid of molecular length/diameter ratio $L^* = L/\sigma = 5$, showed relevant differences in the LC phase diagram with respect to the original Kihara potentials, especially with respect to the stabilization of layered hexatic phases.

The present work provides a more complete evaluation of the potentiality of the GB−K fluid as mesogenic model. For this purpose, we have extended the characterization of the LC phase diagram to molecular systems with different aspect ratios and anisotropy of the dispersive interactions. Particular attention is devoted to the stability of the nematic phase and of layered fluid-like smectic and crystal-like hexatic phases. The investigation aims to contribute to the elucidation of the roles played by the molecular shape and the anisotropy of the dispersive interactions in mesogenic behavior. Such a study seems timely after the recent revisions of the global LC phase diagram of the ellipsoidal GB fluid,[14,15] which constitutes an optimum benchmark for the present work. Valuable information can be obtained from the comparison of the LC phase diagrams and structural properties of GB−K and GB fluids with the same aspect ratios and parametrization of the interaction energy. In this way, the effects imposed by the spherocylindrical and the ellipsoidal cores of these two fluids, respectively, can be unveiled.

The next Section of the paper briefly reviews the definition of the GB−K interaction model and relevant aspects of the Monte Carlo simulation method. The paper then follows with a detailed discussion of the LC phase diagrams for different molecular parametrizations.

II. Method

II.A. Interaction Model. The GB−K potential model is built by incorporating the orientational prefactor of the Gay−Berne potential to the 12-6 Kihara potential.[26] The interaction potential is defined by the following expressions, with the parameter definitions outlined in Table 1:

$$U_{GB-K}(\mathbf{r}_{ij}, \hat{\mathbf{u}}_i, \hat{\mathbf{u}}_j) = \epsilon_{GB}(\hat{\mathbf{r}}_{ij}, \hat{\mathbf{u}}_i, \hat{\mathbf{u}}_j) U_K(d_m) \quad (1)$$

$$U_K(d_m) = 4\epsilon[(\sigma/d_m)^{12} - (\sigma/d_m)^6] \quad (2)$$

$$\epsilon_{GB}(\hat{\mathbf{r}}_{ij}, \hat{\mathbf{u}}_i, \hat{\mathbf{u}}_j) = \epsilon_{GO}(\hat{\mathbf{u}}_i, \hat{\mathbf{u}}_j)^{\nu}[\epsilon'(\hat{\mathbf{r}}_{ij}, \hat{\mathbf{u}}_i, \hat{\mathbf{u}}_j)]^{\mu} \quad (3)$$

$$\epsilon_{GO}(\hat{\mathbf{u}}_i, \hat{\mathbf{u}}_j) = [1 - \chi^2(\hat{\mathbf{u}}_i \cdot \hat{\mathbf{u}}_j)^2]^{-1/2} \quad (4)$$

$$\epsilon'(\hat{\mathbf{r}}_{ij}, \hat{\mathbf{u}}_i, \hat{\mathbf{u}}_j) = 1 - \frac{\chi'}{2}\left[\frac{(\hat{\mathbf{r}}_{ij} \cdot \hat{\mathbf{u}}_i + \hat{\mathbf{r}}_{ij} \cdot \hat{\mathbf{u}}_j)^2}{1 + \chi'(\hat{\mathbf{u}}_i \cdot \hat{\mathbf{u}}_j)} + \frac{(\hat{\mathbf{r}}_{ij} \cdot \hat{\mathbf{u}}_i - \hat{\mathbf{r}}_{ij} \cdot \hat{\mathbf{u}}_j)^2}{1 - \chi'(\hat{\mathbf{u}}_i \cdot \hat{\mathbf{u}}_j)}\right] \quad (5)$$

The spherocylindrical symmetry (a cylinder capped by hemispheres on both ends, see Figure 1) of the molecular core arises from the explicit dependence of the pair potential on d_m. This variable represents the minimum distance between the rigid cores of the molecules, which is an implicit function of the relative center-of-mass positions and orientations of both particles. The prefactor ϵ_{GB} depends explicitly on the three-vector correlations between the directors of the given pair of particles ($\hat{\mathbf{u}}_i$, $\hat{\mathbf{u}}_j$) and the intermolecular center-of-mass vector ($\hat{\mathbf{r}}_{ij}$). The interaction anisotropy is characterized by the usual Gay−Berne four parameter set (κ, κ', ν, and μ) (see Table 1). In particular, $\epsilon_{GB} = 1$ for the crossed configuration, where $\hat{\mathbf{u}}_i \hat{\mathbf{u}}_j = \hat{\mathbf{r}}_{ij} \hat{\mathbf{u}}_j = \hat{\mathbf{r}}_{ij} \hat{\mathbf{u}}_j = 0$. The attractive energy well of a parallel pair of molecules in the side-to-side configuration is κ' times, $\{1 - \chi^2\}^{-\nu/2}$ times and $\{1 - \chi^2\}^{-\nu/2}\{1 - \chi'\}^{-\mu}$ times deeper than for the head-to-tail, crossed and T-shaped configurations, respectively (e.g., see Figure 1 of ref 26). The parameter κ denotes the molecular aspect ratio, which in the spherocylindrical GB−K model is related to the rod length/diameter ratio through $\kappa = L^* + 1$.

The present investigation scopes GB−K fluids with the set of interaction parameters $\kappa' = 20$, $\mu = 1$, and $\nu = 1$ and three aspect ratios, $\kappa = 4.4$, 5, and 6 (i.e., $L^* = 3.4$, 4, and 5). Such choice of parameters, together with our previous study of the GB−K fluid with $\kappa = 6$, $\kappa' = 5$, $\mu = 2$, and $\nu = 1$,[26] allows us to investigate qualitative changes in the LC phase diagram of the fluid with respect to both molecular length and interaction anisotropy. In addition, the chosen parameters provide a link with previous systematic studies for the GB fluid.[14,15] Throughout the paper, the notation GB−K(κ, κ', μ, ν) introduced in previous works[14,26] will be employed. For computing efficiency, the interaction potential is truncated at a distance $d_m = d_C =$

3σ, and shifted so that the energy U_{GB-K} vanishes at the truncation boundary.[26]

Figure 1 compares the overall spherocylindrical shape of the molecules in the GB−K model with the ellipsoidal shape of the GB potential for one of the set of parameters employed in the present work. This Figure also serves to illustrate that the GB−K model resembles, qualitatively, the main features of the multiple-site Lennard-Jones chain potential.

II.B. Monte Carlo Simulations. The isothermal−isobaric ensemble Monte Carlo (NPT−MC) simulation methodology employed to evaluate the liquid crystal phase diagram of the GB−K fluid was essentially the same described in our previous paper.[26] Isobars were run for systems of $N_p = 1492$ molecules at reduced pressures in the range $P^* = P\sigma^3/\epsilon = 0.1-8.0$ (note that a different reduction of pressure, namely $P\sigma^3/k_BT$, was used in ref 26). Simulations for larger systems, with $N_p = 6144$ and 12288, were also performed to elucidate the structure of the layered phases. For each isobar, the stability of isotropic (I), nematic (N), smectic A (Sm A), and hexatic (Hex) phases was explored. This implied covering a range of temperatures within $T^* = k_BT/\epsilon = 0.4-5.0$, depending on the fluid pressure and the molecular elongation. In the reduced expressions for P^* and T^* above, ϵ is the potential energy scaling parameter of $U_K(d_m)$ (eq 2), which corresponds in particular to the well depth for the crossed pair configuration.

Each state was typically equilibrated over 10^6 NPT−MC cycles and ensemble averages of the thermodynamic and structural properties of the system were computed over 3×10^5 cycles. Each MC cycle consisted of N_p attempts for displacements and/or reorientations of randomly chosen particles plus a trial change of the box volume. Volume changes were attempted by randomly changing the length of the each side of the box independently, with the restriction that none of them could become shorter than twice the $L + 3\sigma$ range of the interaction potential. The usual acceptance ratios and periodic boundary conditions are employed.

The calculation of each isobar was started from an equilibrated configuration at low-temperature well inside the hexatic region. Such configuration was built from hexagonal crystal lattices with AB and ABC stacked arrangements[20] or, alternatively, from imperfect hexatic crystal configurations obtained from the cooling of initially disordered fluids. The system was then melted by sequential heating from the hexatic configuration through the different LC phases down to the isotropic phase. Efforts were directed toward the microscopic characterization of the hexatic phase. The disjunctive of assigning a crystal-like structure, or rather a fluid-like smectic B structure, to this phase has been a matter of discussion.[14,28] We will refer to this phase as *hexatic* and will discuss this topic later in the paper. In any case, it was found that the melting temperature of the hexatic phase to the corresponding subsequent smectic A, nematic, or isotropic phase was independent of the type of configuration (AB, ABC, or imperfect crystal) initially assumed for the hexatic phase.

The LC transitions observed during the isobaric heating of the fluid are characterized by discontinuities in density, energy, and in the nematic order and in the bond hexagonal order parameters.[26,29] In addition, sudden qualitative changes in the appropriate radial correlation functions are monitored.[13,15,21,24,26] In particular, the set of functions $g_{1m}(r_\perp)$ was computed, which account for the correlation between a particle in a given smectic layer, with a second particle *m* layers apart, as a function of the component of the pair distance vector perpendicular to the nematic director, $r_\perp$.[15] Such approximate procedure for the estimation of liquid crystal phase boundaries is reliable for the purposes of the present work and has been extensively employed in the past for similar fluids of prolate molecules.[21,23,24,26] A more precise evaluation of the phase diagram should include an accurate calculation of the free energy in each of the phases (e.g., see ref 28), which is beyond the scope of the present study.

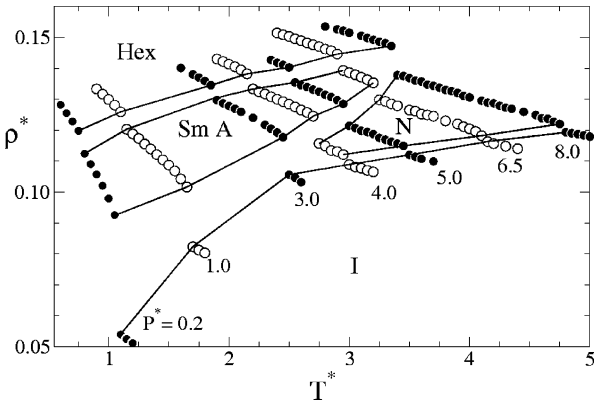

Figure 2. Liquid crystal phase diagram of the GB−K(6, 20, 1, 1) fluid. Stable isotropic (I), nematic (N), smectic A (Sm A), and hexatic (Hex) phases are found. The phase diagram is derived from the Monte Carlo isobaric equations of state (density $\rho^* = \rho\sigma^3$ *versus* temperature $T^* = k_B\,T/\epsilon$) shown in the plot (symbols), for the pressures within $P^* = P\sigma^3/\epsilon = 0.2-8$ indicated next to each curve. The solid lines guide the eye along the boundary of stability of each phase.

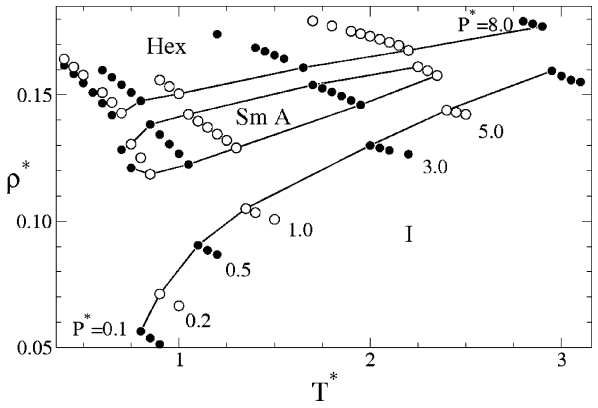

Figure 3. Same as Figure 2 for the GB−K(5, 20, 1, 1) fluid. Stable isotropic (I), Smectic A (Sm A), and Hexatic (Hex) phases are found for this fluid. Note the absence of the nematic phase in the phase diagram.

III. Results

Figures 2−4 show representative isobaric equations of state computed for the GB−K fluids considered in the present study. The different isobars were obtained from the melting of an imperfect hexatic crystal state (see Section II.B). These results serve to illustrate the overall liquid crystalline phase diagram displayed by the Gay−Berne−Kihara fluid, featuring isotropic, nematic, smectic A, and hexatic phases. As it is well-known, the isotropic phase corresponds to a disordered fluid, the nematic phase to a fluid with a net collective alignment of the molecules, the smectic A phase to molecules organized in fluid-like layers of aligned molecules, and the hexatic phase to a crystal-like layered structure with strong interlayer correlations as will be shown below.

A first inspection of the phase diagram of the GB−K(6, 20, 1, 1) fluid (Figure 2) already reveals that the stability of the four observed phases is strongly dependent on the temperature and pressure of the fluid. For temperatures up to $T^* = 2.5$ or

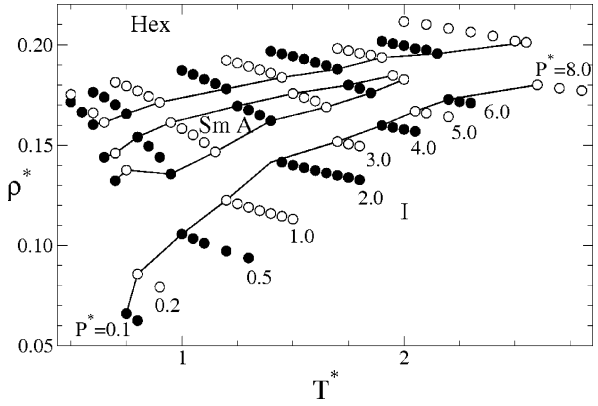

Figure 4. Same as Figure 2 for the GB−K(4.4, 20, 1, 1) fluid. Stable Isotropic (I), Smectic A (Sm A), and Hexatic (Hex) phases are found for this fluid. Note the absence of the nematic phase in the phase diagram, which is in contrast with the Gay−Berne fluid with same aspect ratio and interaction parameters.[15]

pressures up to $P^* = 3$, the GB−K(6, 20, 1, 1) fluid presents only isotropic, smectic A, and hexatic phases. At intermediate temperatures and pressures (within $2.5 < T^* < 3.2$, $3 < P^* < 8$), a more complete sequence of mesophases is found including the nematic phase. Finally, at higher temperatures and pressures, the smectic A phase eventually becomes unstable giving rise to a nematic−hexatic transition. Hence, the simulations lead to a I−N−Sm A triple point at $T^* \approx 2.5-2.6$, $P^* \approx 3-4$, and a N−Sm A−Hex triple point at $T^* \approx 3.2-3.3$, $P^* \approx 7-8$. The simulation results also suggest that an additional I−Sm A−Hex triple point may arise in the limit of small temperature and pressure. This aspect becomes more apparent in the phase diagrams of the GB−K fluids with smaller aspect ratios that will be presented below.

The changes in the energy per particle, the nematic order parameter, and the hexatic bond order parameter[26,29] along the isobars of the GB−K(6,20,1,1) fluid are illustrated in Figure 5. The isobars at $P^* = 1$, 5, and 8 selected for this plot are representative of the three types of phase transition sequences observed for this fluid, namely I−Sm A−Hex, I−N−Sm A−Hex, and I−N−Hex, respectively. The evolution of the nematic order parameter, S_2, and the hexatic bond order parameter, H_6, illustrated in Figure 5, monitor the orientational and positional order in each phase of the fluid. S_2 displays the typical sudden jump to values above 0.6 at the I−N transition and further grows with cooling. Remarkably, in the absence of a stable Sm A phase, as in the $P^* = 8.0$ isobar, the nematic phase reaches S_2 values as large as ≈0.9. The appearance of such strong nematic alignment in the absence of an external field can be expected to be of practical interest. In the Sm A phase, S_2 values within 0.7−0.8 (e.g., for $P^* = 5.0$) or above 0.9 (e.g., for $P^* = 1.0$) can be obtained depending on thermal fluctuations. The transition to the hexatic phase involves, in all cases, an increase in S_2 to values close to unity and a marked discontinuity in H_6 related to the appearance of positional order with a long-range hexagonal packing of the molecules, which is absent in the Sm A phase. A more detailed insight into the structure of the smectic A and hexatic phases is provided at a later stage of the paper in the light of the analysis of specific correlation functions.

Figure 5 shows that the energy per particle grows with temperature at any given pressure. It is of particular interest to note the substantial energetic stabilization of the fluid in the transitions from the isotropic or nematic phase to the smectic A or hexatic phases. Such transitions are also associated to the greatest discontinuities in density. A sizable jump in energy is

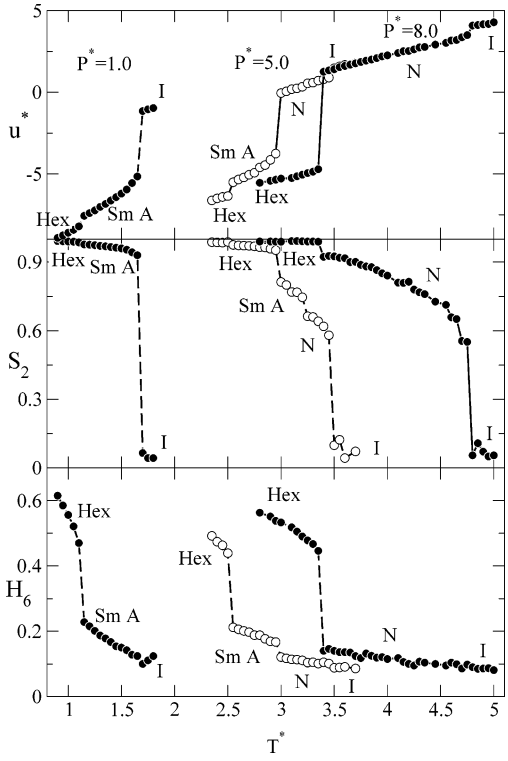

Figure 5. Average interaction energy per particle, $u^* = u/\epsilon$ (Top), nematic order parameter S_2 (middle), and Hexatic bond order parameter H_6 (bottom), along the isobars $P^* = 1$, 5 and 8 of the GB−K(6, 20, 1, 1) fluid. These isobars illustrate the three types of phase transition sequences observed for this fluid, namely I−Sm A−Hex, I−N−Sm A−Hex, and I−N−Hex.

further observed at the Hex−Sm A transition, which follows from the more energetically efficient molecular configuration of the hexatic packing. Additional relevant information about the energetic contribution to the stability of the layered phases can be obtained if the present phase diagram of the GB−K(6, 20, 1, 1) fluid just discussed is compared to similar diagrams of related fluids with smaller anisotropy in the dispersive interactions. The most extreme case is that of the 12-6 Kihara fluid of the same aspect ratio, formally equivalent to the GB−K(6, 1, 0, 0) fluid, in which the dispersive interactions depend only on d_m (i.e., $\epsilon_{GB} \equiv 1$, so that the 12-6 potential energy applies uniformly around the molecular core). The phase diagram of the 12-6 Kihara fluid[23,26] displays a particularly weak dependence of the density of the I−N−Sm A transitions with temperature, which is in contrast with the appreciable increase in the density of the transition lines with increasing temperature in the GB−K(6, 20, 1, 1) fluid (Figure 2). More interestingly, the 12-6 Kihara fluid lacks hexatic- or crystal-like phases in the range of pressures and temperatures presently investigated, which already demonstrates the preponderance of the energetic contributions to the free energy over the entropic ones in the stabilization of the hexatic phase. In this context, it is also enlightening to confront the phase diagram of the GB−K(6, 20, 1, 1) fluid with that obtained in our previous work for the GB−K(6, 5, 2, 1) fluid (Figure 2 of ref 26). In this latter fluid, the energy ratios of the parallel side-to-side pair configuration with respect to the head-to-tail and T-shape configurations are 4-fold smaller than in the parametrization of the present work, whereas the ratio with respect to the crossed configuration is maintained. Noticeably, the phase diagram of the GB−K(6, 5, 2, 1) fluid features a I−N−Sm A triple point very close in temperature and density ($T^* \approx 2.5$, $\rho^* \approx 0.11$) to the one found

for the GB−K(6, 20, 1, 1) fluids. The main difference between the liquid crystal behavior of the two models is related to the enhanced stability of the Sm A phase with respect to the hexatic phase in the less anisotropic GB−K(6, 5, 2, 1) fluid. In fact, the smectic phase was present in the whole range of temperatures investigated in ref 26 and no evidence for a N−Sm A−H triple point was found at temperatures up to $T^* = 5$, which is in contrast to the presence of such a triple point for the GB−K(6, 20, 1, 1) fluid at $T^* \approx 3.3$. One further relevant difference between the two parametrizations of the GB−K model is that in the GB−K(6, 20, 1, 1) fluid the I−N transition is delayed toward greater densities with respect to the GB−K(6, 5, 2, 1) fluid. Although this result was not necessarily expected, it can be traced back to the reduced attractive interactions in the GB−K(6, 20, 1, 1) fluid for configurations of parallel particles away from the side-to-side arrangement. For instance, the head-to-tail pair configuration is four times more attractive in the GB−K(6, 5, 2, 1) fluid than in the GB−K(6, 20, 1, 1) fluid, which results in more negative average potential energies in the nematic phase of the former fluid.

We move on now to the discussion of the phase diagrams obtained for GB−K fluids of smaller molecular aspect ratios, namely $\kappa = 5$ and 4.4 (i.e., $L^* = 4$ and 3.4). The motivation for studying systems of shorter molecules is at least three-fold. First of all, the investigation of different aspect ratios is required to provide a systematic description of the mesogenic behavior of any model fluid. In addition, it is interesting to follow the reference provided by the extensive investigation of the HSC fluid[20,21] which showed qualitative changes in the liquid crystal phase diagram with κ. Finally, the most detailed studies of the GB fluid have been performed for small aspect ratios ($\kappa < 5.0$). In particular, thorough investigations have been carried out for the GB(4.4, 20, 1, 1) fluid,[14,15] and it is of interest to compare its behavior to that of its spherocylindrical counterpart, namely the GB−K(4.4, 20, 1, 1) fluid.

Figures 3 and 4 depict the computed isobaric equations of state and the corresponding phase diagrams GB−K(5, 20, 1, 1) and GB−K(4.4, 20, 1, 1) fluids. One of the most relevant features of both phase diagrams is the absence of the nematic phase. In addition, the island shape of the region of stability of the Sm A phase is even more apparent than for the $\kappa = 6$ fluid. Hence, the simulations suggest the existence of two I−Sm A−H triple points, one at low temperature ($T^* < 0.6$) and a second one at high-temperature ($T^* \approx 2.4$ and 2.1 for $\kappa = 5$ and 4.4, respectively). For even shorter molecules, the smectic A phase can be expected to vanish and, in fact, a shift toward higher densities with an appreciable decrement in the area of the density−temperature diagram corresponding to this phase is already observed in going from $\kappa = 6$ to $\kappa = 4.4$.

These results for the GB−K fluid are in qualitative concordance with the behavior of the hard spherocylinder fluid. For instance, the representation of the phase diagram of the HSC fluid against molecular length displays a I−N−Sm A triple point at $\kappa = 4.7$ (i.e., $L^* = 3.7$) and a I−Sm A−K triple point (K stands for a crystal phase) at $\kappa \approx 4.1$ (i.e., $L^* \approx 3.1$).[20,21] However, some differences are apparent on quantitative grounds. For the GB−K fluids presently investigated, the nematic phase is no longer stable for $\kappa = 5$ and the I−N−Sm A triple point is necessarily located at a greater aspect ratio than in the HSC fluid, within $\kappa = 5-6$. Furthermore, the analogous I−Sm A−K triple point, although not explicitly investigated here, can be expected to arise in the GB−K fluid at values appreciably smaller than $\kappa = 4.1$, since for $\kappa = 4.4$, the smectic phase is still stable over a significant region of densities and temperatures (see Figure 4). Such differences can be attributed to the specific energetic contribution added in the GB−K fluid, on top of the excluded volume steric effects that to can be considered similar for the two fluids.

The phase diagram of the GB−K(4.4, 20, 1, 1) was computed partly with the aim to establish a comparison between the spherocylindrical GB−K fluid and the ellipsoidal Gay−Berne fluid. The GB(4.4, 20, 1, 1) fluid presents stable isotropic, nematic, smectic and hexatic phases[14,15] and thus displays a phase diagram qualitatively different from that of the GB−K(4.4, 20, 1, 1) fluid (Figure 4). In fact, the phase diagram of the GB(4.4, 20, 1, 1) system resembles the features found here for the GB−K(6, 20, 1, 1) fluid (Figure 2). Interestingly, the investigations of the Gay−Berne model have shown that it leads to stable nematic phases under a broad range of molecular aspect ratios and interaction parameters. The nematic phase was found to be stable in the GB fluid with $\kappa = 3$, which to our knowledge constitutes the smallest aspect ratio for which mesogenic behavior has been explored for this model.[12] It is important to notice that in the purely repulsive ellipsoidal models, such as the hard ellipsoid fluid, the only stable liquid crystalline phase is the nematic phase.[7] Smectic phases become stable only if specific attractive interactions are introduced in the model. Consequently, in models with ellipsoidal symmetry the nematic phase appears to be inherently stabilized by the molecular shape, so that this phase remains stable for significantly smaller aspect ratios in comparison to their spherocylinder fluid counterparts. For instance, the hard ellipsoid fluid presents a stable nematic phase down to aspect ratios as small as $\kappa \approx 2.5$,[30] in comparison to $\kappa \approx 4.1$ for the hard spherocylinder fluid.[20,21]

A relevant topic in the context of the present study is the elucidation of the structures of the nematic, smectic, and hexatic phases of the GB−K fluid and their comparison with those of related model fluids, namely the HSC and the GB fluids. The most relevant features of the structural character of each of these LC phases can be projected into appropriate pair distribution functions capturing the positional and orientational correlation of the particles.[26,29] Figure 6 depicts a first set of correlation functions commonly employed in liquid crystal studies. The radial distribution function, $g(r^*)$, is qualitatively similar in the isotropic and nematic phases, where it shows little structure apart from the void for $r^* = r/\sigma < 1.0$ and some smooth short-range oscillations. With the appearance of the positional order in the layered Sm A and Hex phases, the radial distribution function displays a substantial increment in its short-range structure as well as appreciable oscillations at longer ranges, which reflect the efficient packing of the roughly parallel particles in the layered arrangement. The depression observed in $g(r^*)$ at intermediate distances ($r^* = 3.5-6.0$ in Figure 6) is associated to the depletion of particle centers of mass in the interlayer region. The radial distribution of the hexatic phase state shows a double-peak structure in the second or greater coordination shells directly associated to the hexagonal crystalline ordering of the molecules within each layer (see also Figure 5).

The layered structure of the Sm A and Hex phases reveals itself more clearly through the long-range positional correlations with respect to the nematic director vector of the system. Figure 6 illustrates this by means of the distribution functions along the nematic director, $g_{||}(r^*_{||})$, and the inlayer distribution, $g_{11}(r^*_{\perp})$. Since the nematic director is aligned with the normal of the layers, $g_{||}(r^*_{||})$ displays oscillations with the period of the interlayer spacing. The double-peak structure in $g_{11}(r^*_{\perp})$ differentiates the Hex phase from the Sm A phase in a similar but sharper way than the radial distribution $g(r^*)$.

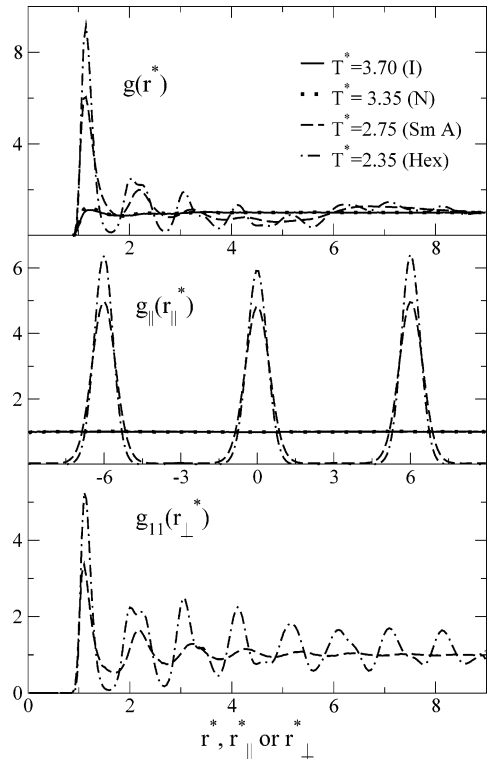

Figure 6. Distribution functions for the GB−K(6, 20, 1, 1) fluid in the isotropic phase ($P^* = 5$, $T^* = 3.70$), nematic phase ($P^* = 5$, $T^* = 3.35$), smectic A phase ($P^* = 5$, $T^* = 2.75$), and hexatic phase ($P^* = 5$, $T^* = 2.35$). Top panel: Radial distribution functions, $g(r^*)$; Middle panel: distribution function along the nematic director $g_{||}(r^*_{||})$ for the Sm A and Hex states. Bottom panel: Inlayer distribution function $g_{11}(r^*_{\perp})$ for the Sm A and Hex states.

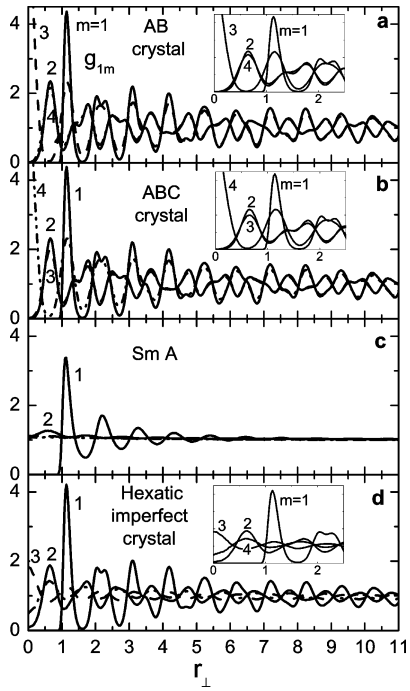

Figure 7. Inlayer and interlayer distribution functions, $g_{1m}(r^*_{\perp})$ ($m = 1, 2, 3, 4$) for a Sm A state ($P^* = 4$, $T^* = 1.8$) and for different Hexatic configurations ($P^* = 4$, $T^* = 1.6$) of the GB−K(4.4, 20, 1, 1) fluid. (a) Hex state obtained from the heating of a perfect AB crystal; (b) Hex state obtained from the heating of a perfect ABC crystal; (c) Sm A state obtained from the melting of the fluid from the Hex phase; (d) Hex state obtained from the freezing of the fluid from the Sm A phase. All computations were performed with systems of 6144 particles arranged in six layers.

There has been certain controversy regarding whether the analogous hexatic phases found in GB fluids correspond to either (fluid) Sm B phases[14] or rather to crystalline (AB or ABC) phases.[15] To investigate this aspect in detail, we performed systematic computations of the Hex and Sm A phases of the GB−K fluid with systems of 6144 and 12 288 particles. The simulations were started at low temperature from 6-layer or 12-layer configurations, respectively, of a perfect AB or ABC solid. The crystalline structure was then heated at constant pressure over a number of states through the Hex−Sm A transition and well inside the Sm A phase. No difference in these simulations with 6144 and 12 288 particles were observed that could be attributed to system size effects. For each state, the interlayer correlation functions $g_{1m}(r^*_{\perp})$ with $m = 1-4$ were specifically inspected. Illustrative results are shown in Figure 7 for the GB−K(4.4, 20, 1, 1) fluid at $P^* = 4$. At this pressure the Hex−Sm A transition takes place at $T^* = 1.70-1.75$ (Figure 4). The relative stability of the AB and ABC crystals is not of major concern within the context of the present investigation. The difference in free energy between both crystal arrangements is too subtle and their microscopic configurations are too far away from each other in the phase space to draw conclusions from the Monte Carlo method employed here. In fact, in our simulations the fluid retains the structure of the initial AB or ABC crystal through the hexatic phase all the way down to the Hex−Sm A transition. Figure 7 (panels a and b) depicts the strong and qualitatively different crystal-like correlations between the layers maintained in the AB and ABC hexatic phases at $T^* = 1.60$, a temperature already close to the boundary with the Sm A phase. It can be noted that the g_{13} of one crystal type is similar to the g_{14} function of the other type. Nevertheless, the two types of crystals melted to the Sm A transition at the same temperature. Once in the Sm A phase, the layers become fluid-like and the interlayer correlations consequently vanish, as can be observed in Figure 7c. The Sm A state does not retain memory about the structure of the Hex phase from which it was melted.

At this point, it seemed natural to freeze the Sm A fluid back to the Hex phase to test whether the long-range intralayer and interlayer correlations observed for the crystal phases (AB or ABC) would be reconstructed or if, on the contrary, it would lead to a smectic B phase with only short-range correlations. Figure 7d shows the $g_{1m}(r^*_{\perp})$ correlation functions for the $T^* = 1.60$ hexatic state resulting from the sequential freezing of the GB−K(4.4, 20, 1, 1) fluid through the Sm A−Hex transition at $T^* = 1.70$. As can be observed, the hexatic phase formed in this way keeps a strong inlayer correlation (g_{11}) and also between nearest-neighboring layers (g_{12}), both of which closely resemble the long-range structure found for the AB and ABC crystals. In particular, the g_{12} distribution features a negligible probability density at $r^*_{\perp} \approx 0$ and a differentiated peak at $r^*_{\perp} \approx 0.5$. The physical interpretation of this finding is straightforward: the interdigitation of the hemispherical caps of the particles exposed at the surfaces of adjacent layers. Note that such interdigitation constitutes a fundamental qualitative difference with respect to the Sm A phase for which virtually no interlayer correlation is present.

Figure 7d also shows that the g_{13} and g_{14} distribution functions present an appreciably weaker structure than the crystal arrangements (Figure 7a, b). The computations for this hexatic state were extended over 10^6 Monte Carlo cycles, which represented a CPU (1.6 GHz) computation time of the order of 2 months. In spite of the long simulation runs, the structure in

g_{13} and g_{14} never became more pronounced than for the case depicted in Figure 7d. It can be noted that these distributions display shallow maxima at positions associated to an AB stacked arrangement. This is, however, not necessarily indicative of the evolution of the system toward a thermodynamically stable AB crystal. The inspection of the hexatic molecular arrangement revealed that the relative configuration of a given layer with respect to layers $m = 3$ and 4 can be described as a mixture of domains of AB type with domains of ABC type. The result is an imperfect crystal-like configuration in which the average interlayer correlations are diminished.

In summary, the long-range correlations observed in $g_{11}(r_{\perp}^*)$ and $g_{12}(r_{\perp}^*)$, together with the interpretation in terms of defects of the weaker correlations in $g_{13}(r_{\perp}^*)$ and $g_{14}(r_{\perp}^*)$, are consistent with the assignment of a crystalline character to the hexatic phase displayed by the GB−K fluids scoped in the present work. For the Gay−Berne GB(4.4, 20, 1, 1) fluid it was similarly concluded, after a systematic revision of the phase diagram from simulation and free-energy calculations,[15,28] that the smectic B phase originally proposed was actually unstable with respect to the solid crystalline phase. It was argued that the freezing of the GB fluid to the hexatic phase from a less ordered phase (Sm A, N, or I) in a Monte Carlo iterative procedure systematically led to an imperfect crystal arrangement with long-range correlations midway between a true crystal and a smectic B. Such arrangement was then likely to be misassigned to this latter phase.

To our knowledge, the only investigations of hexatic phases in spherocylindrical fluid models have been performed by Aoki and co-workers,[31,32] McGrother and co-workers,[21] Bolhuis and Frenkel,[20] and our group.[26] A sizable first-order Sm B-crystal transition was reported by Aoki for perfectly parallel soft repulsive molecules with aspect ratio $\kappa = 2$. On the other hand, McGrother[21] and Bolhuis[20] reported on a stable crystal phase for HSC fluids with $\kappa = 4-6$, without any evidence for domains of stability of a Sm B phase. Our results for the GB−K fluid are consistent with these latter investigations, and extend the domain of stability of the hexatic phase due to the favorable energetics. For the shorter particles with purely repulsive interactions investigated by Aoki, a stable Sm B phase could be interpreted as a consequence of the smaller steric constrains imposed on the layers.

IV. Conclusions and Final Remarks

We have presented a systematic study of the liquid crystal phase behavior of a coarse-grain prolate spherocylindrical model with attractive and repulsive pair interactions dependent on orientation. The so-called GB−K potential was introduced in a recent work[26] and provides a more realistic description of the overall shape of real mesogens in comparison to the ellipsoidal Gay−Berne potential. The topology of the interactions in the GB−K model resembles the main features of the multiple-site Lennard-Jones chain potential.

Monte Carlo simulations in the isobaric−isothermal ensemble have been performed for GB−K fluids of different elongation and interaction parameters favoring parallel pair orientations. Three types of triple points are observed in the phase diagrams, namely I−Sm A−Hex, I−N−Sm A and N−Sm A−Hex. The GB−K model leads to a stronger dependence of the qualitative features of the phase diagram on temperature in comparison to the more conventional Kihara fluids. It is observed that the nematic phase becomes only stable for molecules of sufficiently high aspect ratio, so that for $\kappa < 6$ the liquid crystal behavior of the fluid is dominated by the layered phases. Furthermore, the Sm A phase presents island-like domains of stability. In fact, the anisotropy of the dispersive interactions introduced in the GB−K model reduces the range of stability of the nematic and smectic phase in favor of the hexatic phase.

The hexatic phase displayed by the different GB−K fluid models scoped in our work features long-range correlations and is therefore identified as a crystalline phase rather than as a fluid-like Smectic B phase. This is in agreement with previous results for HSC fluids of similar aspect ratios.[20,21] The freezing of the fluid from the Sm A phase to the hexatic phase leads to an imperfect solid. The correlations between the molecules in the same layer or in the nearest-neighboring layer remain as strong and long-ranged as in a perfect crystal. On the other hand, the presence of defects in the crystal structure lead to mixed domains of AB and ABC stacking, which effectively reduces the average overall correlations between molecules two or more layers apart. The simulation results are inconclusive with respect to the relative stability of the AB and ABC stacking arrangements of the crystal. Similar effects have been responsible for the revision of the initial assignment of Sm B phases in the GB fluid, currently recognized as crystal phases.[15,28] Smectic B phases reported for repulsive spherocylinder fluids of short molecules ($\kappa = 2$)[31,32] are likely to be stable, as a consequence of the smaller orientational steric constraints.

Some appreciable differences become apparent between the phase diagrams of the (spherocylindrical) GB−K and the (ellipsoidal) GB fluid of same aspect ratio and interaction parameters. In particular, the GB model inherently provides an enhanced stability of the nematic phase with respect to the smectic and crystal phases even for short molecules with $\kappa < 3$.[12]

It can be concluded that the GB−K fluid model characterized in detail in this work and in ref 26 provides an effective coarse-grain approach to real mesogenic systems. The model corrects one fundamental pitfall of the conventional Kihara fluid, namely the lack of an explicit dependence of the pair interaction on the relative orientation of the molecules. The GB−K fluid can be viewed as an alternative to the well-known Gay−Berne fluid, introducing the more realistic molecular core shape in a straightforward way. The effect of each type of molecular symmetry (spherocylindrical or ellipsoidal) on the relative stability of the nematic, smectic and crystal phases has been outlined in the present work. It should serve to guide the choice of fluid model when drawing interpretations and predictions for actual mesogens.

Acknowledgment. B.M.H. acknowledges support from the Regional Government of Andalusia (projects P06-FQM-0189 and FQM-205) and the Ministry of Education and Science of Spain (project CTQ2004-07730-C02). A.C. acknowledges support from the Nederlandse Organisiate voor Wetenschappelijk Onderzoek (NWO).

References and Notes

(1) Allen, M. P.; Tildesley, D. J. *Computer Simulation of Liquids*; Clarendon Press: Oxford, 1987.

(2) Frenkel, D.; Smit, B. *Understanding Molecular Simulation*; Academic Press: London, 1996.

(3) Wilson, M. *Rev. Phys. Chem.* **2005**, *24*, 421.

(4) Care, C. M.; Cleaver, C. J. *Rep. Prog. Phys.* **2005**, *68*, 2665.

(5) Lebwohl, P. A.; Lasher, G. *Phys. Rev. A* **1972**, *6*, 426.

(6) Zannoni, C. J. *Mater. Chem.* **2001**, *11*, 2637.

(7) Frenkel, D.; Lekkerkerker, H. N. W.; Stroobants, A. *Nature* **1988**, *332*, 822.

(8) Berne, B. J.; Pechukas, P. *J. Chem. Phys.* **1972**, *56*, 4213.

(9) de Miguel, E.; del Rio, E. M. *J. Chem. Phys.* **2003**, *118*, 1852.

(10) Barmes, F.; Cleaver, D. J. *Phys. Rev. E* **2005**, *71*, 021705.
(11) Gay, J. G.; Berne, B. J. *J. Chem. Phys.* **1981**, *74*, 3316.
(12) Rull, L. F. *Physica A* **1995**, *220*, 113.
(13) Brown, J. T.; Allen, M. P.; del Rio, E. M.; de Miguel, E. *Phys. Rev. E* **1998**, *57*, 6685.
(14) Bates, M. A.; Luckhurst, G. R. *J. Phys. Chem.* **1999**, *110*, 7087.
(15) de Miguel, E.; del Rio, E. M.; Blas, F. J. *J. Chem. Phys.* **2004**, *121*, 11183.
(16) Padilla, P.; Velasco, E. *J. Chem. Phys.* **1997**, *106*, 10299.
(17) de Miguel, E.; del Rio, E. M. *J. Chem. Phys.* **2001**, *115*, 9072.
(18) del Rio, E. M.; de Miguel, E. *Phys. Rev. E* **2005**, *71*, 051710.
(19) Kihara, T. *J. Phys. Soc. Jpn.* **1951**, *16*, 289.
(20) Bolhuis, P.; Frenkel, D. *J. Chem. Phys.* **1997**, *106*, 666.
(21) McGrother, S. C.; Williamson, D. C.; Jackson, G. G. *J. Phys. Chem.* **1996**, *104*, 6755.
(22) Earl, D. J.; Ilnytskyi, J. M.; Wilson, M. R. *Mol. Phys.* **2001**, *99*, 1719.
(23) Cuetos, A.; Martínez-Haya, B.; Lago, S.; Rull, L. F. *Phys. Rev. E* **2003**, *68*, 011704.
(24) Cuetos, A.; Martínez-Haya, B.; Lago, S.; Rull, L. F. *J. Chem. Phys.* **2002**, *117*, 2934.
(25) Cuetos, A.; Martínez-Haya, B.; Lago, S.; Rull, L. F. *J. Phys. Chem. B* **2005**, *109*, 13729.
(26) Martínez-Haya, B.; Cuetos, A.; Lago, S.; Rull, L. F. *J. Chem. Phys.* **2005**, *122*, 024908.
(27) Vesely, F. J. *J. Chem. Phys.* **2006**, *125*, 214106.
(28) de Miguel, E.; Vega, C. *J. Chem. Phys.* **2002**, *117*, 6313.
(29) Zewdie, H. *Phys. Rev. E* **1988**, *57*, 1793.
(30) Allen, M. P. In *Observation, Prediction and Simulation of Phase Transitions in Complex Fluids*, Proceedings of the NATO Advanced Study Institute, Varenna, Italy, July 25−August 5, 1994; Baus, M., Rull, L. F., Ryckaert, J.-P., Eds.; Kluwer Academic Publishers: Dordrecht, 1995; p 557.
(31) Aoki, K. M.; Yonezawa, F. *Phys. Rev. Lett.* **1992**, *69*, 2780.
(32) Aoki, K. M.; Yonezawa, F. *Phys. Rev. A* **1992**, *46*, 6541.